

SYNTHESIS AND CHARACTERIZATION OF SUCROSE AND GLUCURONIC ACID-CAPPED CdS NANOPARTICLES FROM HDA-CAPPED VIA LIGAND EXCHANGE

M. J. MOLOTO^{a*}, P. M. SHUMBULA^b

^a*Department of Chemistry, Vaal University of Technology, Private Bag X021, Vanderbijlpark, 1900, South Africa*

^b*Advanced Materials Division, Mintek, Private Bag X3015, Randburg, 2125, South Africa*

Hexadecylamine (HDA) or trioctylphosphine oxide (TOPO) was employed to stabilize CdS nanoparticles using single-source precursor route which resulted in the formation of rods, bipods and tripods. The complex, cadmium diethyldithiocarbamate was first dissolved trioctylphosphine (TOP) before injecting into hot HDA or TOPO solution. This in turn made the particles stabilized by HDA or TOPO soluble in organic solvents such as toluene. Ligand exchange was employed to replace HDA or TOPO with sucrose and glucuronic acid in order to make the nanoparticles water soluble. The stabilizing molecule, HDA is known to promote non-spherical shapes especially rods and this combined with the nature of the precursor yielded non-spherical particles. However, the above was not the same with TOPO as a capping molecule with spherical shapes being observed from the TEM images. Blue shifts were observed for particles capped by HDA, sucrose and glucuronic acid. The photoluminescence spectra showed red shifts in relation to the absorption band edges. Powder X-ray diffraction (PXRD) pattern showed the hexagonal phase of the CdS nanoparticles. Fourier transform infrared (FT-IR) spectroscopy was also used to confirm the successful removal of HDA or TOPO molecules on the surface of nanoparticles and replaced by the hydroxyl and carbonyl groups of sucrose and glucuronic acid.

(Received December 3, 2016; Accepted March 2, 2017)

Keywords: CdS nanorods; cadmium complex; quantum dots; water-soluble

1. Introduction

Quantum dots (QDs) are semiconductor nanocrystals with a diameter range of 1-10 nm [1,2]. These QDs are constituted of different compounds or groups such as II-VI, III-V or IV (Si, Tin). Most reports in the past decade have been on group II-VI than others. The semiconductor nanocrystals are excitons confined in all three spatial dimensions. As a result, they have properties that are between those of bulk semiconductors and those of discrete molecules. Many scientists are interested in the quantum size effect [3], and the promising applications of semiconductor nanocrystals in light-emitting diodes [4, 5], solar cells [6], catalysis [7] and others. Of all the other types of materials, the group II-VI semiconducting materials such as CdS, ZnS, etc., are more attractive due to their large band gaps that can be tuned. However, it has been reported that QDs of group III-V elements are more stable than group II-VI elements, which is due to covalent bond rather than ionic bond character [8], although group III-V semiconductor nanomaterials are difficult to prepare.

Generally organic molecules are used in stabilizing nanoparticles and also controlling nucleation and growth of particles in order to prevent agglomeration [9]. These molecules include surfactants, which are composed of a polar head group and of one or more hydrocarbon chains, which form hydrophobic part. During the synthesis, the surfactants are continuously adsorbing and desorbing from the surface of the nanocrystals through their headgroups, permitting the crystals to

*Corresponding author email: makwenam@vut.ac.za

grow in controlled way [10, 11]. Nanoparticle growth is kinetically controlled in many situations, where multiple interacting parameters simultaneously determine final nanoparticle size and shape [12]. Therefore, simply replacing one solvent or capping molecule by another does not guarantee products with similar chemical and physical features [13]. Critical factors such as temperature and time have been consciously preferred to control the size and morphology of the nanoparticles since the properties of the nanoparticles. The most evident manifestation of properties is the optical light emission in the blue – red spectral region analyzed by a blue-shift at smaller crystallite dimensions [14].

Quantum dots are also known to be more attractive to biological applications because of their small size and dimensional similarity to biological molecules such as proteins, DNA, peptides and nucleic acids [15 - 18]. Organic dyes are used for biological applications such as biolabeling, but they have many drawbacks such as narrow absorption spectra, broad emission spectra, instability and weak photobleaching, while QDs are the opposite [19, 20]. Quantum dots synthesized from single source precursor route [21, 22], are generally coated with water insoluble organic molecules. Different strategies have been employed to convert hydrophobic nanoparticles to hydrophilic ones and that includes ligand exchange [23 - 25], hydrophobic interaction [26, 27] and silica encapsulation [28]. Brunchez *et al.* [29] and Pellegrino *et al.* [30] reported that methods for solubilisation without affecting vital properties are mostly based on exchange of the original hydrophobic surfactant layer with a hydrophilic one, or the introduction of a second layer which may also contain another functional group.

In this work, we report the synthesis of diethyldithiocarbamate cadmium (II) complex as single source precursor for the preparation of HDA or TOPO-capped CdS nanoparticles. These HDA or TOPO capping molecules are substituted in further reactions by sucrose and glucuronic acid making water soluble CdS nanoparticles.

2. Experimental section

2.1. General

The capping molecules, HDA (hexadecylamine), sucrose and glucuronic acid as well as TOP (trioctylphosphine) which was also used as precursor solvent, were purchased from Aldrich and used without further purification. Cadmium chloride, sodium diethyldithiocarbamate trihydrate (analytical grade) obtained from Aldrich. Solvents such as methanol, hexane, chloroform, pyridine and ethylacetate, were also purchased from Aldrich and used as obtained. Toluene was purchased from Aldrich and was dried in molecular sieves. The complex was prepared using the method described in the literature [31, 32].

2.2. Characterization

Microanalysis was performed on a CARLO ERBA elemental analyzer for C, H, N and S. Optical absorption measurements were carried out using an Analytikjena SPECORD 50 UV-visible spectrophotometer, and the samples were placed in quartz cuvettes (1-cm path length), using toluene and distilled water as reference solvents. Emission spectra of the particles were recorded on a Perkin Elmer LS 45 photoluminescence (PL) spectrometer with a xenon lamp at room temperature. The samples were placed in glass cuvettes (1 cm). X-ray diffraction (XRD) analysis were carried out on a Phillips X'Pert materials research diffractometer using secondary graphite monochromated Cu K α radiation ($\lambda=1.5406 \text{ \AA}$) at 40 KV/50 mA. Samples were supported on glass slides. Measurements were taken using a glancing angle of incidence detector at an angle of 2θ , for 2θ values over $10-80^\circ$ in steps of 0.05° with a scan speed of $0.01^\circ 2\theta \text{ s}^{-1}$. Infrared spectra of ligand, complex, hydrophobic and hydrophilic nanoparticles were recorded on Bruker Optics Tensor 27. Transmission electron microscope (TEM) measurement was performed on a Philips CM120 BIOTWIW electron microscope operating at 80 kV. Samples for TEM measurements were prepared by spreading a drop of dilute dispersion of the as-prepared products on copper grids and then dried in air.

2.3. HDA-capped CdS nanoparticles

Hexadecylamine (HDA) (4 g, 16.56 mmol) or TOPO (6 g, 16.56 mmol) was heated to about 120 °C or 180 °C in a three-necked flask in an inert atmosphere. A precursor (1.00 g, 2.45 mmol) was dispersed in 5 ml of TOP, and then the solution was injected into the hot HAD or TOPO while stirring, causing temperature of the reaction mixture to drop by 15 to 20 °C. Heating was continued to recover the temperature (120 °C or 180 °C), and then maintained for 1 h. The solution was then cooled to *ca.* 70 °C and an excess amount of methanol was added. The flocculent precipitate formed was centrifuged and the supernatant was decanted, then the isolated solid was dispersed in toluene. Toluene was removed by using rotary evaporator and excess methanol added to remove excess HDA or TOPO. The above centrifugation and isolation procedure was then repeated three times for the purification of the prepared CdS nanocrystals.

2.4. Sucrose and glucuronic acid-capped CdS nanoparticles

To a three-necked flask, 1 g of HDA or TOPO-capped CdS was added into 5 ml (61.82 mmol) of pyridine. The mixture was stirred for an hour at room temperature. Hexane (20 ml) was then added to precipitate nanoparticles which were isolated by centrifugation. The supernatant was then decanted. A solution of either sucrose or glucuronic acid in methanol (20 ml) was added to a three-necked flask containing a mixture of CdS nanoparticles and methanol (10 ml). The mixture was stirred for 2 h at 40 °C and then overnight at room temperature or 2 h at 80 °C. Chloroform, ethyl acetate and diethyl ether were added to precipitate nanoparticles. Nanoparticles were then centrifuged and the supernatant decanted.

3. Results and discussion

The single source precursor route produces particles with well controlled size distribution by using very air and moisture stable complexes, which are also easy to prepare and often producing high yield of good quality crystalline nanoparticles. The preparation of the precursor required the use of cadmium chloride as a metal source and diethyldithiocarbamate salt as a sulphide source [31, 32]. The reaction was prepared in 1:2 mol ratio of the salt and the ligand by stirring for 2 h at room temperature. The complex was characterised by elemental analysis and spectroscopic techniques.

3.1. Infrared spectra

Fig. 1 represents the IR spectral data for (a) HDA, (b) sucrose and (c) glucuronic-acid capped CdS nanoparticles. The C-N vibration peak at 1464 cm^{-1} and C-H peak at 1570 cm^{-1} are due to hexadecylamine. The N-H asymmetric peak at 3233 cm^{-1} is weak due to the amine ligand bound to the nanocrystal surface. Other prominent bands that are significant in determining the presence of amine ligands, which are due to C-H stretching bands, are observed at 2849 cm^{-1} and 2914 cm^{-1} (Figure 1 (a)). This observation demonstrates that QDs are stabilized by hexadecylamine. These observations were also reported by Meulenberg *et al.* [33]. In Figure 1 (b) and (c), the broad bands of valence (symmetrical and asymmetrical) oscillations of OH at 3301 and 3366 cm^{-1} , C-H at 2908 and 2823 cm^{-1} observed are due to the presence of sucrose and glucuronic acid. The well-defined band appearing at 1699 cm^{-1} corresponds to valence vibration of the carbonyl group.

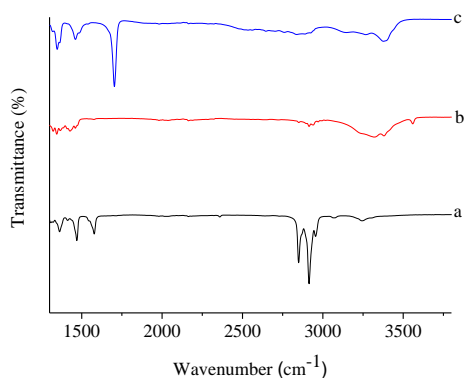


Fig. 1. FTIR spectra of CdS nanoparticles capped by (a) HDA (120 °C), (b) sucrose (RT), (c) glucuronic acid (RT) synthesized from diethyldithiocarbamate cadmium complex.

To further elucidate whether pods were obtained due to the precursor used, thermolysis was also performed at 180 °C using TOPO as the capping agent instead of HDA. Confirmation of the presence of the capping agent (TOPO) on the surface of the nanomaterial was also investigated using infrared spectroscopy (Figure 2). TOPO is known to absorb strongly at 1146 and 1466 cm⁻¹ corresponding to P=O stretching and CH₂ bending, respectively. In the spectrum of CdS nanoparticles capped by TOPO (Figure 2), the P=O stretching vibration peak centered at 1141 cm⁻¹ and CH₂ bending peak at 1462 cm⁻¹ have moved to lower wavenumbers.

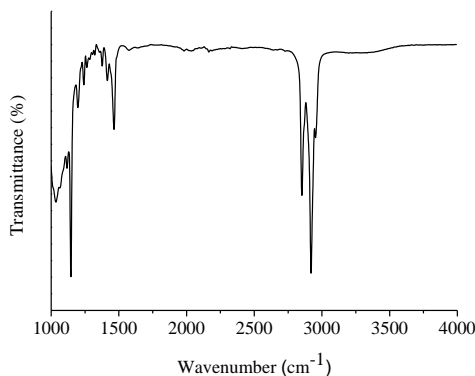


Fig. 2. FTIR spectrum of CdS nanoparticles capped by TOPO (180 °C) synthesized from diethyldithiocarbamate cadmium complex

3.2. Optical properties

Thermolysis of Cd[(C₂H₅)₂NCS₂]₂ in hexadecylamine was carried out at 120 °C for an hour, while the reactions of sucrose and glucuronic acid-capped CdS nanoparticles were run at room temperature. The main feature on the properties of QDs is their band gap, the energy separation between the filled valence band and the empty conduction band. All the absorption spectra in Figure 3I (a), (b) and (c) show band edges that are blue shift to bulk CdS (515 nm (2.41 eV)), which signify small sizes of the nanoparticles. The band edge of HDA-capped, sucrose-capped and glucuronic acid-capped CdS nanoparticles is 491 (2.53 eV), with excitonic peaks positioned at 458 nm (2.71 eV).

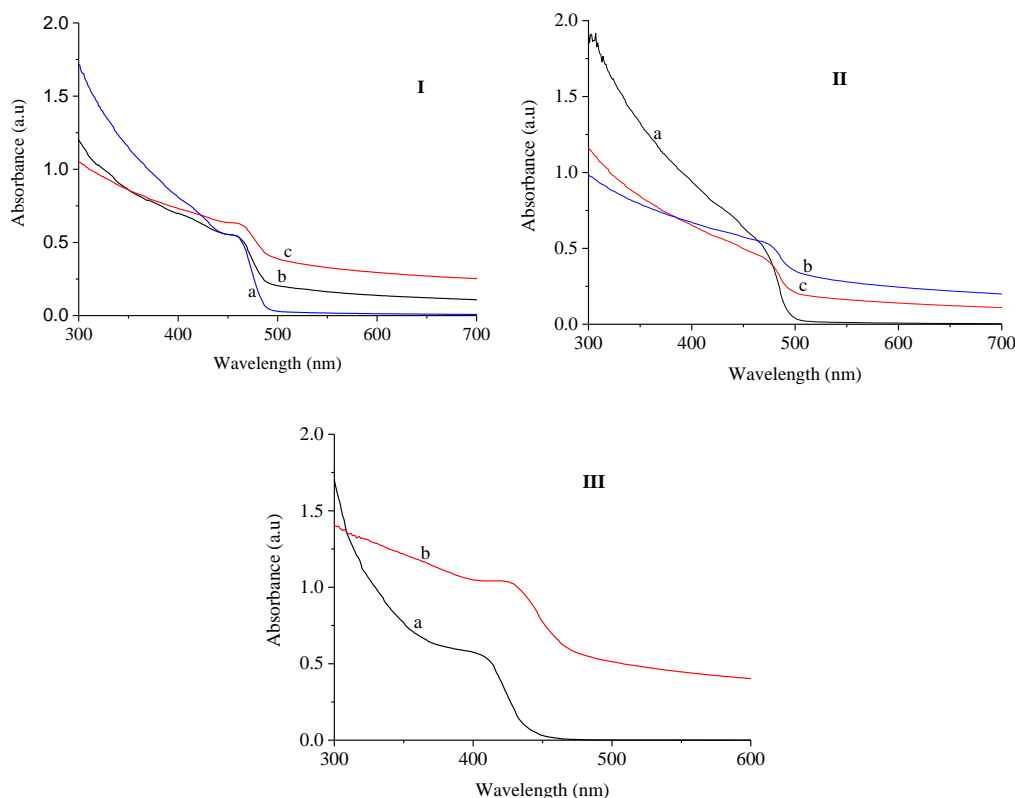


Fig. 3. Absorption spectra of CdS nanoparticles capped by (I) (a) HDA (120 °C), (b) sucrose (RT), (c) glucuronic acid (RT), (II) (a) HDA (180 °C), (b) sucrose and (c) glucuronic acid, (III) (a) TOPO (180 °C) and (b) glucuronic acid (80 °C) synthesized from diethyldithiocarbamate cadmium complex.

The photoluminescence spectrum of the bulk CdS has been reported to have a broad emission maximum in the region 500–700 nm [34]. The narrow photoluminescence or emission spectra (excitation at 300 nm) in Figure 4I(a)-(c) have an emission maxima appearing at 484 nm (2.56 eV). All the emission spectra (Figure 4I-III) are red shifted to their absorption spectra. To confirm the effect of temperature on the preparation of CdS nanoparticles, the same precursor was employed at 180 °C. The reaction was also run for an hour. Although the absorption and emission spectra (Figures 3II and 4II) behaved similar to the ones reported above, they were observed to have slightly shifted to lower energy with the band edge appearing at 502 nm (2.47 eV) while the excitonic peaks appear at 475 nm (2.61 eV). The emission spectra, which are broader than the CdS synthesized at 120 °C, have a maximum absorption peaks positioned at 494 nm (2.51 eV). Sucrose and glucuronic acid which were used as capping molecules or agents, are soluble in water and also biocompatible.

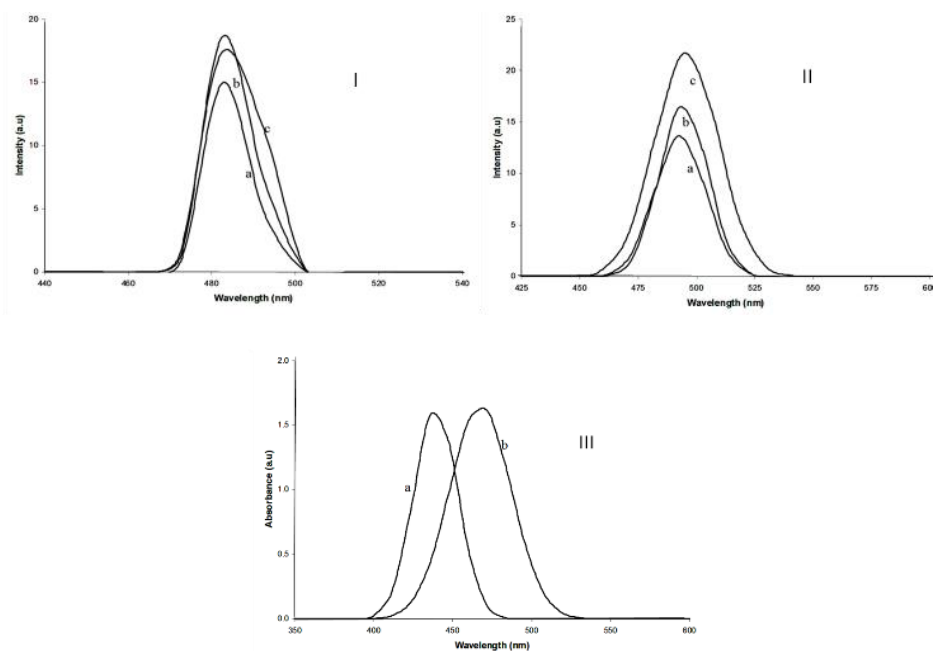


Fig. 4: Photoluminescence spectra of CdS nanoparticles capped by (I) (a) HDA (120 °C), (b) sucrose (RT), (c) glucuronic acid (RT), (II) (a) HDA (180 °C), (b) sucrose and (c) glucuronic acid, (III) (a) TOPO (180 °C) and (b) glucuronic acid (80 °C) synthesized from diethyldithiocarbamate cadmium complex.

The absorption spectra of CdS nanoparticles capped by TOPO and glucuronic acid (Figure 3II & III) are also blue shift compared to the CdS bulk, with their photoluminescence spectra (Figure 4II & III) being red shift to their as-prepared absorption spectra. However, the absorption and emission spectra of CdS nanoparticles capped by glucuronic acid prepared from CdS nanoparticles capped by TOPO have shifted to higher wavelength, which is lower energy. This has been caused by the temperature employed, which is 80 °C instead of room temperature as explored above when preparing water soluble nanoparticles. This temperature was employed to speed up the process instead of performing overnight or long time reactions.

3.3. Structural properties

Fig. 5 (a), (b) and (c) depict the TEM images of CdS nanoparticles capped by HDA, sucrose and glucuronic acid, respectively, under different conditions. All the images show particles with a range of rod-shaped particles, i.e., from monorods, bipods to tripods as observed more clearly on HDA and glucuronic acid-capped CdS nanoparticles (Figure 5 (a) and (c)). Although rod shapes are still maintained for sucrose-capped CdS nanoparticles image (Figure 5 (b)), the particles appear to lose their sharp edges, with signs of rods collapsing into short rods as compared to TEM images of CdS capped by HDA and glucuronic acid. The particles diameters as determined from the TEM images lie in the range of 3.8 to 5.7 nm. However, as the temperature is increased, more bi- and tripods are formed as can be clearly observed in Figure 6(a). The formation of this type of rods is not new as was reported before. Li *et al.* [35] thermolysed cadmium ethylxanthate $\{Cd(C_2H_5OCS_2)_2\}$ and reported the formation of four armed, three armed and two armed rods. The formation of two armed and three armed rods augurs well with our results, except the four armed ones, which were not observed in our case.

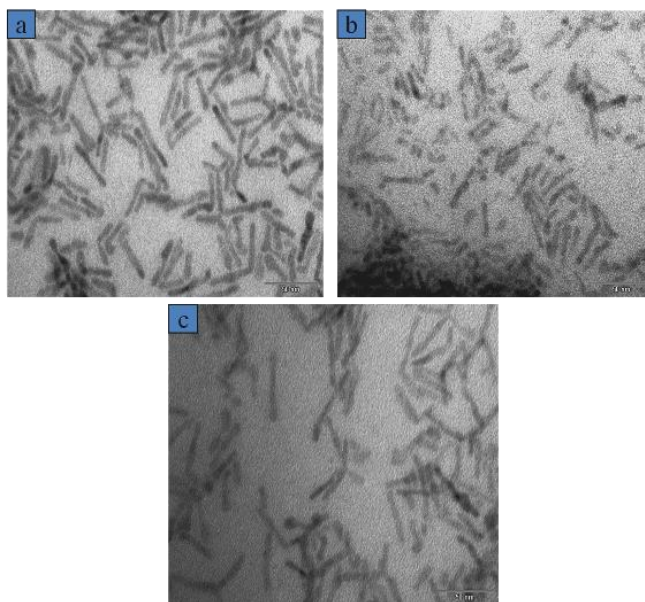


Fig. 5: TEM images (scale bar: 50 nm) of CdS nanoparticles capped by (a) HDA (120 °C), (b) sucrose (room temperature) and (c) glucuronic acid (room temperature)

The particles diameters as determined from the TEM images (180 °C and room temperature) are in the range of 4.4 to 6.7 nm. However, there are signs of particles collapse in the sucrose and glucuronic acid-capped CdS nanoparticles. The rod shape image for HDA-capped CdS nanoparticles confirms the report by L. Manna *et al.* [35] who reported that single chain surfactant molecules, such as primary alkyl amines tend to favour rods particles.

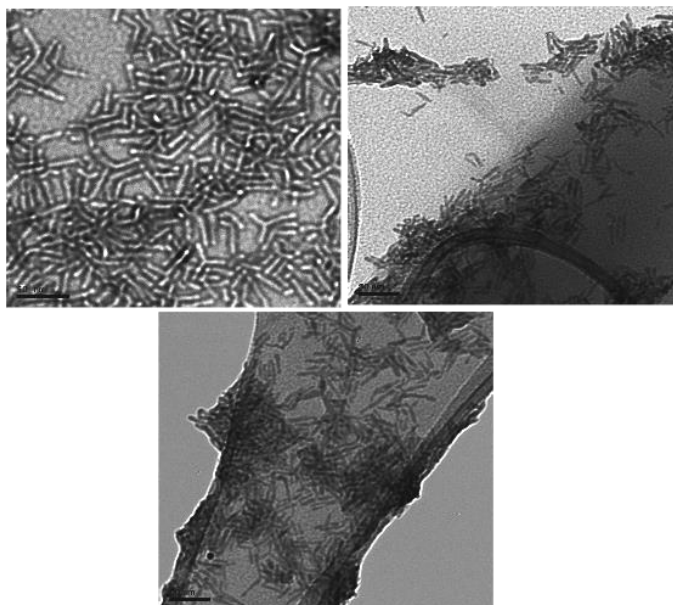


Fig. 6. TEM images (scale bar: 50 nm) of CdS nanoparticles capped by (a) HDA (180 °C), (b) sucrose (room temperature) and (c) glucuronic acid (room temperature)

It is interesting to note that the shape of the nanoparticles did not change as a result of temperature. Both TEM images of CdS nanoparticles capped by TOPO and glucuronic acid (Figure 7) depict spheres particles in shape as a result of the capping agent, which is TOPO. However, although spheres were obtained, sizes for the particles differed for CdS nanoparticles capped by TOPO (Figure 7 (a), average size: 2.6 nm) and those capped by glucuronic acid, with

bigger particles for glucuronic acid capped CdS nanoparticles (Figure 7 (b), average size: 4.2 nm). This augurs well with the absorption and emission spectra that shifted to higher wavelength. This indicates that for transfer of hydrophobic nanoparticles to hydrophilic nanoparticles, room temperature should be employed if particles of almost the same size need to be maintained.

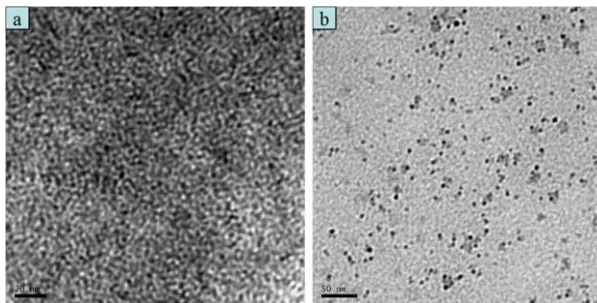


Fig. 7. TEM images (scale bar: (a) 20 nm and (b) 50 nm) of CdS nanoparticles capped by (a) TOPO (180 °C) and (b) glucuronic acid (80 °C) from diethyldithiocarbamate cadmium complex

Figure 8a depicts the XRD pattern of HDA-capped CdS nanoparticles prepared at 120 °C for 1 h. The broad peaks observed at 2-Theta or θ values 26.6°, 26.9°, 28.5°, 35.9°, 44.2°, 48.2° and 52.3°, indexed to 100, 002, 101, 102, 110, 103 and 110 planes for hexagonal phase, respectively. The broadening of the peaks indicates the finite size of the particles. The CdS nanoparticles capped with sucrose and glucuronic acid were also analysed with XRD (not shown here). Both graphs showed multiple peaks which might have overlapped with CdS nanoparticles peaks. Figure 8b shows the XRD pattern of CdS nanoparticles capped by HDA synthesized at 180 °C. Similar observations (Figure 8a) were noticed. However, the peaks, especially 110, 103 and 112 are slightly narrower than the CdS 120 °C but broader than bulk CdS, which support the TEM results on a slightly bigger particles. The presence of the (110), (103) and (112) planes from both diffraction patterns is characteristic of the wurtzite or hexagonal phase CdS. The stronger and narrower (002) peak in contrast to other peaks, indicating that the sample or material is elongated along the *c*-axis.

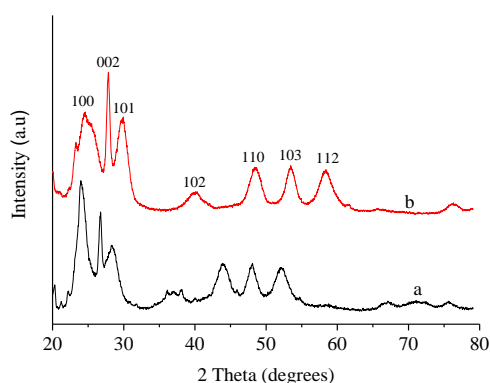


Fig. 8. XRD pattern of CdS nanoparticles capped by HDA (prepared at 120 °C (a) and 180 °C (b) synthesized from diethyldithiocarbamate cadmium complex.

4. Conclusions

CdS nanoparticles prepared from the complex, cadmium diethyldithiocarbamate were synthesized and characterized to show blue shifts in relation to the bulk. The resulting HDA, sucrose and glucuronic acid-capped CdS nanoparticles which range from 3.8 to 5.7 nm and 4.4 to

6.7 nm in diameter, with TOPO and its glucuronic acid-capped CdS ranging from 2.6 to 4.2 nm. The obtained diameters show a strong quantum confinement effect. The HDA-capped CdS properties as compared to the sucrose and glucuronic capped showed no marked difference except for the TEM image which shows the tendency for surface interaction changing from the NH to OH group of the organic molecules stabilizing them. However, optical properties of TOPO and its glucuronic acid-capped CdS nanoparticles showed some differences which were due to temperature. The XRD pattern of CdS nanoparticles capped by HDA showed wurtzite or hexagonal phase. The substitution of the HDA or TOPO (water insoluble) rendered them water soluble and retained the optical properties, an almost essential part for the biolabeling.

Acknowledgements

This work was supported by funding from University of Witwatersrand, and National Research Foundation, South Africa. Thanks are due to Dr. PM Shumbula for his contribution to the work.

References

- [1] C. B. Murray, C. R. Kagan, M. G. Bawendi, *Ann. Rev. Mater. Res.*, **30**, 545, (2000).
- [2] A. M. Smith, G. Ruan, M. N. Rhyner, S. Nie, *Annals of Biomedical Engineering*, **34**, 3 (2006).
- [3] L. E. Brus, *J. Chem. Phys.* **90**, 2555, (1986).
- [4] M. C. Schlamp, X. G. Peng, A. P. Alivisatos, *J. Appl. Phys.* **82**, 5837, (1997).
- [5] S. Coe, W. K. Woo, M. Bawendi, V. Bulovic, *Nature*, **420**, 800 (2002).
- [6] W. Huynh, J. J. Dittmer, A. P. Alivisatos, *Science*, **295**, 225 (2002).
- [7] T. S. Ahmadi, Z. L. Wang, T. C. Green, A. Henglein, M. A. Elsayed, *Science*, **272**, 1924 (1996).
- [8] M. A. Malik, P. O'Brien, M. Helliwell, *J. Mater. Chem.*, **15**, 1463 (2005).
- [9] C. B. Murray, D. J. Norris, M. G. Bawendi, *J. Am. Chem. Soc.*, **115**, 8706 (1993).
- [10] S. M. Lee, S. N. Cho, J. Cheon, *Adv. Mater.*, **15**, 441 (2003).
- [11] Y. W. Jun, S. M. Lee, N. J. Kang, J. Cheon, *J. Am. Chem. Soc.* **123**, 5150 (2001).
- [12] M. L. Steigerwald, L. E. Brus, *Acc. Chem. Res.*, **23**, 183 (1990).
- [13] C. J. Murphy, *J. Mater. Chem.*, **18**(19), 2161 (2008).
- [14] R. Rossetti, L. Ellison, J. M. Gibson, L. E. Brus, *J. Chem. Phys.*, **80**(9), 4464 (1984).
- [15] S. R. Whaley, D. S. English, E. L. Hu, P. F. Barbara, A. M. Belcher, *Nature* **405**, 665 (2000).
- [16] R. Elghanian, J. J. Storhoff, R. C. Mucic, R. L. Letsinger, C. A. Mirkin, *Science* **227**, 1078 (1997).
- [17] G. P. Mitchell, C. A. Mirkin, R. L. Letsinger, *J. Am. Chem. Soc.*, **121**, 8122 (1999).
- [18] S. Pathak, S. K. Choi, N. Arnheim, M. E. Thompson, *J. Am. Chem. Soc.* **123**, 4103 (2001).
- [19] J. Aldana, Y. A. Wang, X. Peng, *J. Am. Chem. Soc.* **123**, 8844 (2001).
- [20] W. Guo, J. J. Li, Y. A. Wang, X. Peng, *Chem. Mater.* **15**, 3125 (2003).
- [21] T. Tridade, P. O'Brien, *Adv. Mater.*, **8**, 161 (1996).
- [22] T. Tridade, P. O'Brien, *Chem. Mater.* **9**, 523 (1997).
- [23] L. Qu, Z. A. Peng and X. Peng, *Nano Lett.*, **1**, 333 (2001).
- [24] H. Mattoussi, J. M. Mauro, E. R. Goldman, G. P. Anderson, V. C. Sundar, F. V. Mikulec, M. G. Bawendi, *J. Am. Chem. Soc.*, **122**, 12142 (2000).
- [25] D. V. Talapin, A. L. Rogach, A. Kornowski, M. Hasse, H. Weller, *Nano Lett.* **1**, 207 (2001).
- [26] W. W. Yu, E. Chang, R. Drezek, V. L. Colvin, *Biochemical and Biophysical Research Communications*, **348**, 781 (2006).
- [27] L. Shen, P. E. Laibinis, T. A. Hatton, *Langmuir*, **15**, 447 (1999).

- [28] D. Gerion, F. Pinaud, S. C. Williams, W. J. Parak, D. Zanchet, S. Weiss, A. P. Allivisatos, *J. Phys. Chem. B.*, **105**, 8861 (2001).
- [29] M. Brunchez, M. Moronne, P. Gin, S. Weiss, A. P. Allivisatos, *Science*, **281**, 2013 (1998).
- [30] T. Pellegrino, L. Manna, S. Kudera, T. Liedl, D. Koktysh, A. L. Rogach, *Nano Lett.*, **4**, 703 (2004).
- [31] T. Trindade, P. O'Brien, *J. Mater. Chem.* **6(3)**, 343 (1996).
- [32] D. Coucouvanis, *Prog. Inorg. Chem.*, **11**, 233 (1970).
- [33] R. W. Meulenbergh, S. Bryan, C. S. Yun, G. F. Strouse, *J. Phys. Chem. B*, **106**, 7774 (2002),.
- [34] N. Chestnoy, T. D. Harris, R. Hull, L. E. Brus, *J. Phys. Chem.*, **90**, 3393 (1986).
- [35] Y. Li, X. Li, C. Yang, Y. Li, *J. Mater. Chem.* **13**, 2641 (2003).
- [36] L. Manna, L. W. Wang, R. Cingolani, A. P. Allivisatos, *J. Phys. Chem. B* **109**, 6183 (2005).